J|A|C|S ARTICLES

Published on Web 03/19/2010

An Active-Site Phenylalanine Directs Substrate Binding and C−H Cleavage in the α-Ketoglutarate-Dependent Dioxygenase TauD

Kevin P. McCusker and Judith P. Klinman*

Departments of Chemistry and Molecular and Cell Biology, and the California Institute for Quantitative Biosciences, University of California, Berkeley, California 94720

Received November 5, 2009; E-mail: klinman@berkeley.edu

Abstract: Enzymes that cleave C−H bonds are often found to depend on well-packed hydrophobic cores that influence the distance between the hydrogen donor and acceptor. Residue F159 in taurine α-ketoglutarate dioxygenase (TauD) is demonstrated to play an important role in the binding and orientation of its substrate, which undergoes a hydrogen atom transfer to the active site Fe(IV)═O. Mutation of F159 to smaller hydrophobic side chains (L, V, A) leads to substantially reduced rates for substrate binding and for C−H bond cleavage, as well as increased contribution of the chemical step to k_{cat} under steady-state turnover conditions. The greater sensitivity of these substrate-dependent processes to mutation at position 159 than observed for the oxygen activation process supports a previous conclusion of modularity of function within the active site of TauD (McCusker, K. P.; Klinman, J. P. *Proc. Natl. Acad. Sci. U.S.A.* **2009**, *106*, 19791−19795). Extraction of intrinsic deuterium kinetic isotope effects (KIEs) using single turnover transients shows 2- to 4-fold increase in the size of the KIE for F159V in relation to wild-type and F159L. It appears that there is a break in behavior following removal of a single methylene from the side chain of F159L to generate F159V, whereby the protein active site loses its ability to restore the internuclear distance between substrate and Fe(IV)═O that supports optimal hydrogenic wave function overlap.

Introduction

The investigation of C−H activation by enzymes has, over a period of several decades, led to the recognition of the importance of quantum mechanical tunneling during the catalyzed transfer of hydrogen from its donor to acceptor sites.[1,2] The ability of an enzyme to ensure efficient hydrogenic wave function overlap[3,4] is intimately linked to two classes of protein motions, termed preorganization and reorganization.[1,5] Preorganization defines the search over a protein's conformational landscape, in order to access a subset of catalytically relevant conformers that contain the requisite, large number of interactions among active-site residues and bound substrates. Within these catalytically viable protein substates, a reorganization barrier defines further transient adjustments in active-site electrostatics and internuclear distances that complete the requirements for barrier penetration.

As would be expected for such a constrained reaction coordinate, the nature of side chain residues that sit behind the bound substrates may be expected to exert considerable influence on catalytic efficiency. An early study of the alcohol dehydrogenase from horse liver (HLADH) focused on a bulky hydrophobic residue (V203) situated behind the nicotinamide ring of the NAD^+ cofactor.[6] Diminution in the bulk of this residue both decreased the rate of hydrogen transfer and altered the properties of the secondary isotope effect.[7,8] Despite the changes in active-site geometry, the magnitude of the primary isotope effect remained largely unaltered.[7,9] This can be rationalized within a gating term that describes the contribution of the sampling of donor−acceptor distances to the reaction barrier; this process generates the final internuclear distance(s) that can maximally support tunneling.[3,4] The impact of site-specific mutagenesis on such distance sampling is two-fold, initially increasing the inter-reactant distance, which then can be restored via an active-site vibration; the latter is facilitated by the reduced vibrational frequency that accompanies the incorporation of a smaller active-site side chain.[3−5]

Another prototypic enzyme system for which systematic changes in active-site packing density have been introduced via site-specific mutagenesis is the non-heme iron enzyme, soybean lipoxygenase (SLO-1). Once again, the focus of mutation was on hydrophobic residues, though in this case, residues both proximal (L546 and L754) and distal (I553) to the C−H bond undergoing cleavage were targeted.[4,10−12] When the two

(1) Nagel, Z. D.; Klinman, J. P. *Nat. Chem. Biol.* **2009**, *5*, 543–550.
(2) Nagel, Z. D.; Klinman, J. P. *Chem. Rev.* **2006**, *106*, 3095–3118.
(3) Kuznetsov, A. M.; Ulstrup, J. *Can. J. Chem.* **1999**, *77*, 1085–1096.
(4) Knapp, M. J.; Rickert, K.; Klinman, J. P. *J. Am. Chem. Soc.* **2002**, *124*, 3865–3874.
(5) Klinman, J. P. *Chem. Phys. Lett.* **2009**, *471*, 179–193.
(6) Ramaswamy, S.; Eklund, H.; Plapp, B. V. *Biochemistry* **1994**, *33*, 5230–5237.
(7) Bahnson, B. J.; Colby, T. D.; Chin, J. K.; Goldstein, B. M.; Klinman, J. P. *Proc. Natl. Acad. Sci. U.S.A.* **1997**, *94*, 12797–12802.
(8) Knapp, M. J.; Meyer, M. P.; Klinman, J. P. In *Hydrogen Transfer Reactions*; Schowen R., Klinman J. P., Eds.; Wiley-WCH Verlag: Weinheim, Germany, 2007; Vol.*4*, pp 1241−1284.
(9) Rubach, J. K.; Ramaswamy, S.; Plapp, B. V. *Biochemistry* **2003**, *42*, 2907–2915.
(10) Meyer, M.; Klinman, J. P. *Chem. Phys.* **2005**, *319*, 283–296.
(11) Knapp, M. J.; Klinman, J. P. *Eur. J. Biochem.* **2002**, *269*, 3113–3121.

10.1021/ja909416z

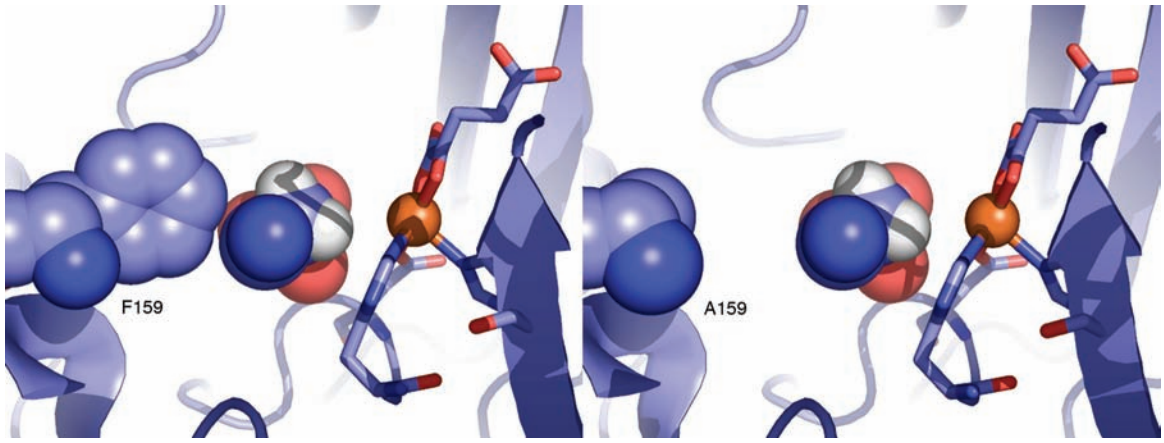

Figure 1. Active site of TauD, illustrated for the WT (left, PDB 1OS7[24]) and the F159A (right, generated in silico[25]).

residues proximal to the reactive position of substrate were converted to alanine, the rate of bond cleavage was significantly reduced while the size of the isotope effect remained close to that of wild-type.[4,10,11] This behavior is similar to that of the HLADH. A somewhat different pattern was seen at position 553, where a progressive reduction in size of the side chain to glycine led to a small, overall ca. 6-fold reduction in rate.[12] Once again, the magnitude of the kinetic isotope effects (KIEs) was largely constant, with the important exception of I553G, where the isotope effect became inflated from ca. 80 at 25 °C with all other mutants to ca. 180.

The α-ketoglutarate (α-KG)-dependent mono- and dioxygenases represent another example of non-heme iron enzymes that catalyze the cleavage of C−H bonds.[13,14] This very large family of enzymes is characterized by an enormous divergence of substrate specificities and primary protein sequences, together with the retention of a similar constellation of inner sphere ligands at the active-site iron.[13,15,16] In all cases investigated, the decarboxylation of α-KG is linked to the production of a high-valent iron-oxo intermediate, which acts as the reactive oxygen species in C−H activation.[17−19] A particularly well-characterized member of this family is the taurine α-ketoglutarate dioxygenase (TauD): where R = H, CH_3.[19−22]

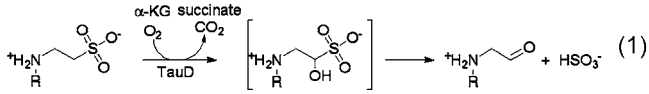

(1)

Using TauD as a prototype, Bollinger and co-workers were the first to provide detailed spectroscopic evidence for the reactive Fe(IV)═O, as well as demonstrating a large primary deuterium isotope effect for the decay of this species in the course of hydrogen atom loss from the substrate taurine.[17,23] In the present study, we turn to site-specific mutagenesis with TauD, targeting a specific phenylalanine (F159) that has been identified from X-ray studies to reside behind the reactive carbon of bound substrate (Figure 1).[24,25] We were particularly interested in the impact of a reduction in bulk of a side chain within an active site that lies very close to the solvent surface. It might be reasoned that the ability of an enzyme to recover from an increase in the hydrogen donor−acceptor distance by way of distance sampling would be circumscribed in such an instance. The study of kinetic deuterium isotope effects in O_2 consuming enzymes can present significant challenges in experimental design and interpretation, due to kinetic uncoupling between the formation of an activated O_2 species and its subsequent reaction with substrate. However, the recent quantification of the extent of O_2/substrate coupling in a series of F159 mutants of TauD, together with the kinetic studies presented herein, provides a reliable estimate of the trend in the kinetic isotope effect as a function of size of the residue at position 159. As shown, TauD is able to tolerate the reduction of side chain from Phe to Leu relatively well, whereas deletion of an additional methylene upon insertion of Val greatly inflates the size of the kinetic isotope effect. This behavior is reminiscent of that seen with SLO-1 mutants, suggesting the limits to which an enzyme's active-site packing can be modified before the onset of highly non-native behavior.

Materials and Methods

General. All reagents were purchased from commercial sources and used without further purification unless otherwise indicated. 1,1-[$^1H_2$] and 1,1-[$^2H_2$]-2-methylaminoethane-1-sulfonic acids were synthesized as previously reported.[26]

Protein Expression/Purification. TauD was expressed and purified as previously reported, with minor modifications.[17,27]

Steady-State Assays. Steady-state rates of oxygen consumption were measured with a YSI model 5300 biological oxygen electrode

(12) Meyer, M. P.; Tomchick, D. R.; Klinman, J. P. *Proc. Natl. Acad. Sci. U.S.A.* **2008**, *105*, 1146–1151.
(13) Costas, M.; Mehn, M. P.; Jensen, M. P.; Que, L. *Chem. Rev.* **2004**, *104*, 939–986.
(14) Hewitson, K. S.; Granatino, N.; Welford, R. W. D.; McDonough, M. A.; Schofield, C. J. *Philos. Trans. R. Soc. London, Ser. A* **2005**, *363*, 807–828.
(15) Hegg, E. L.; Que, L. *Eur. J. Biochem.* **1997**, *250*, 625–629.
(16) Loenarz, C.; Schofield, C. J. *Nat. Chem. Biol.* **2008**, *4*, 152–156.
(17) Price, J. C.; Barr, E. W.; Tirupati, B.; Bollinger, J. M.; Krebs, C. *Biochemistry* **2003**, *42*, 7497–7508.
(18) Hausinger, R. P. *Crit. Rev. Biochem. Mol. Biol.* **2004**, *39*, 21–68.
(19) Bollinger, J. M.; Price, J. C.; Hoffart, L. M.; Barr, E. W.; Krebs, C. *Eur. J. Inorg. Chem.* **2005**, *2005*, 4245–4254.
(20) vanderPloeg, J. R.; Weiss, M. A.; Saller, E.; Nashimoto, H.; Saito, N.; Kertesz, M. A.; Leisinger, T. *J. Bacteriol.* **1996**, *178*, 5438–5446.
(21) Eichhorn, E.; vanderPloeg, J. R.; Kertesz, M. A.; Leisinger, T. *J. Biol. Chem.* **1997**, *272*, 23031–23036.
(22) Bollinger, J. M.; Krebs, C. *J. Inorg. Biochem.* **2006**, *100*, 586–605.
(23) Price, J. C.; Barr, E. W.; Glass, T. E.; Krebs, C.; Bollinger, J. M. *J. Am. Chem. Soc.* **2003**, *125*, 13008–13009.
(24) O'Brien, J. R.; Schuller, D. J.; Yang, V. S.; Dillard, B. D.; Lanzilotta, W. N. *Biochemistry* **2003**, *42*, 5547–5554.
(25) DeLano, W. L. The PyMOL Molecular Graphics System; DeLano Scientific, LLC: Palo Alto, CA, 2008.
(26) McCusker, K. P.; Klinman, J. P. *Tetrahedron Lett.* **2009**, *50*, 611–613.
(27) McCusker, K. P.; Klinman, J. P. *Proc. Natl. Acad. Sci. U.S.A.* **2009**, *106*, 19791–19795.

using *N*-methyltaurine. The choice of *N*-methyltaurine for these studies was based on the ease of synthesis of deuterated isotopologs, together with the similarity of kinetic parameters for *N*-methyltaurine to taurine.[26] The fixed assay conditions were as follows: 50 mM bis-tris (pH 6.2), 100 μM Fe(II)$(NH_4)_2(SO_4)_2$, and 200 μM sodium ascorbate in a volume of 1 mL at 30 °C. The pH of 6.2 was selected to facilitate oxygen uptake measurements, as basic pH values resulted in nonenzymatic oxygen uptake due to oxidation of Fe(II).[27] α-KG was held constant at a saturating concentration of 1 mM, after initial measurements at 1 or 10 mM indicated that 1 mM was saturating in all instances. The substrate, *N*-methyltaurine, was varied from 2 to 10 000 μM and oxygen from 5 to 1100 μM. Enzyme was present in concentrations between 0.1 and 3 μM. The apparent kinetic parameters k_{cat} and K_m were determined by nonlinear fitting of the kinetic data to the Michaelis−Menten equation, using the program KaleidaGraph. The parameter k_{cat} was obtained by extrapolation to infinite concentrations of O_2 and *N*-methyltaurine; K_m for O_2 was determined at a concentration at least 10-fold over K_m (*N*-methyltaurine); K_m for *N*-methyltaurine was determined at ambient O_2 (237 μM), and survey measurements at ~400 μM O_2 gave values within error of those obtained at 237 μM, indicative that 237 μM is sufficiently saturating. We have recently determined the extent of coupling of oxygen uptake to product (sulfite) formation under saturating conditions.[27] This allows us to calculate the steady-state rates of product formation (k_{cat}(prod)) from the rates of oxygen consumption (k_{cat}):

$$k_{cat} \times ([SO_3^{2-}/O_2]) = k_{cat}(\text{prod}) \quad (2)$$

As kinetic isotope effects on k_{cat} are ratios of these rates, this expression can easily be extended to the calculation of steady-state KIEs on product formation ($^Dk_{cat}$(prod)) from observed values ($^Dk_{cat}$):

$$^Dk_{cat} \times \{([SO_3^{2-}/O_2])^H/([SO_3^{2-}/O_2])^D\} = {}^Dk_{cat}(\text{prod}) \quad (3)$$

We have previously noted the absence of additional oxidation products from *N*-methyltaurine when sulfite production is completely uncoupled from O_2 uptake.[27] In the absence of alternative oxidation products, the ratio $[SO_3^{2-}]/[O_2]$ reports directly on the ratio of substrate functionalization to O_2 uptake.

Stopped-Flow Assays. Stopped-flow UV−visible spectra were obtained using a Hi-Tech Scientific model SF-61 DX2 stopped-flow spectrophotometer (xenon lamp, photodiode array detection mode, 1.0 cm path length, 1.5 ms integration time) in single-mixing mode. The system was made anaerobic by flushing the flow system with 50 mM bis-tris buffer, pH 6.2 made anaerobic by repeated vacuum/argon cycles. Enzyme/α-KG/substrate solutions in 50 mM bis-tris buffer were made anaerobic by repeated vacuum/argon cycles; an anaerobic solution of Fe(II), as ferrous ammonium sulfate in water, was added using a gastight syringe. The anaerobic Fe(II) solution was prepared by exchanging the headspace over a Thermo Scientific Reacti-Vial containing ferrous ammonium sulfate with argon and adding an appropriate volume of water sparged vigorously with argon using a gastight syringe. One drive syringe of the stopped-flow apparatus contained 550 μM enzyme, 500 μM Fe(II), 10 mM H or D substrate, and 10 mM α-KG in 50 mM bis-tris buffer pH 6.2. The other contained 50 mM bis-tris buffer saturated with O_2 (1200 μM). These solutions were mixed in a 1:1 ratio. The stopping volume was approximately 100 μL, and the drive pressure was 0.4 MPa. The temperature of the drive syringes and the observation cell were maintained at 10 °C using a Neslab recirculating bath. Apparent rate constants from kinetic traces were calculated from monoexponential fits using Kinetic Studio software (version 1.0.5.19739, TgK Scientific). It should be noted that the decay phases of these traces were fit equally well by a biexponential rise and fall; however, linear data collection precluded good fits to the initial rise due to insufficient early data points. The decay rates were not statistically different when fitted to the two models. Due to the enzymes being saturated with all substrates under stopped-flow conditions, the stoichiometry of product formation to oxygen consumption obtained under saturating steady-state conditions was used to calculate the rate of hydrogen abstraction k_{prod} from k_{decay}, which was determined from fitting experimental data as outlined above. The KIE, $^Dk_{prod}$, was thus determined analogously to $^Dk_{cat}$(prod).

Scheme 1[a]

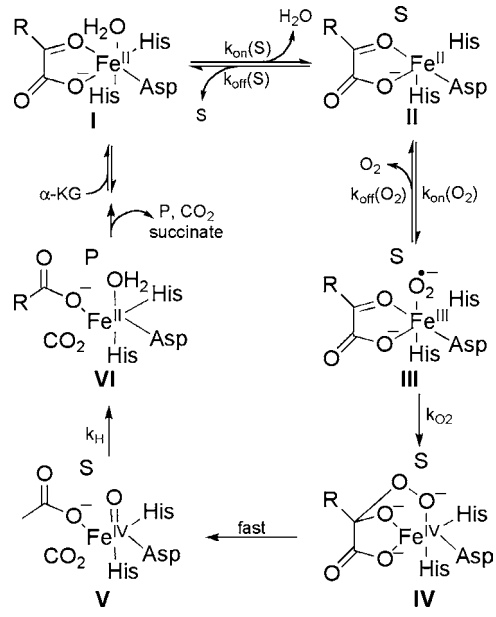

[a] Minimal kinetic mechanism of an Fe^{II}- and α-KG-dependent oxygenase.[13] S represents substrate, P represents product, R = $CH_2CH_2CO_2^-$. Water binding and dissociation have been omitted from the product formation and dissociation steps as well as the α-KG binding step for clarity. Microscopic rate constants discussed in the text are indicated.

Results and Discussion

Steady-State Partial Reaction with Dioxygen. Given the consensus mechanism of TauD involving ordered binding and "substrate triggering" (Scheme 1),[13,17,28] the irreversible activation of oxygen appears in a segment after substrate binding and before C−H activation. The mutations employed for the current study (cf. Figure 1) were designed to impact specifically the substrate-dependent portions of the reaction. The effect of these mutations on the oxygen activation chemistry, thus, provides an important control. Two readily accessible experimental parameters monitor the oxygen activation performed by TauD: the pre-steady-state rate of accumulation of the Fe(IV)═O species and the steady-state parameter $k_{cat}/K_m(O_2)$. In the case of wild-type enzyme, these second-order rate constants are within error of each other, indicative that both parameters are reporting on the same processes.[29] The parameter $k_{cat}/K_m(O_2)$ reflects the binding of oxygen through the first irreversible step, the formation of the peroxohemiketal (species IV in Scheme 1).

$$k_{cat}/K_m(O_2) = (k_{O_2} \times k_{on}(O_2))/(k_{O_2} + k_{off}(O_2)) \quad (4)$$

Reciprocal plots of $1/v$ versus $1/O_2$ are presented in Figure 2A to illustrate graphically the changes in slope that occur in proceeding from WT to F159A. The corresponding values for

(28) Hanauske-Abel, H. M.; Gunzler, V. *J. Theor. Biol.* **1982**, *94*, 421–455.
(29) Price, J. C.; Barr, E. W.; Hoffart, L. M.; Krebs, C.; Bollinger, J. M. *Biochemistry* **2005**, *44*, 8138–8147.

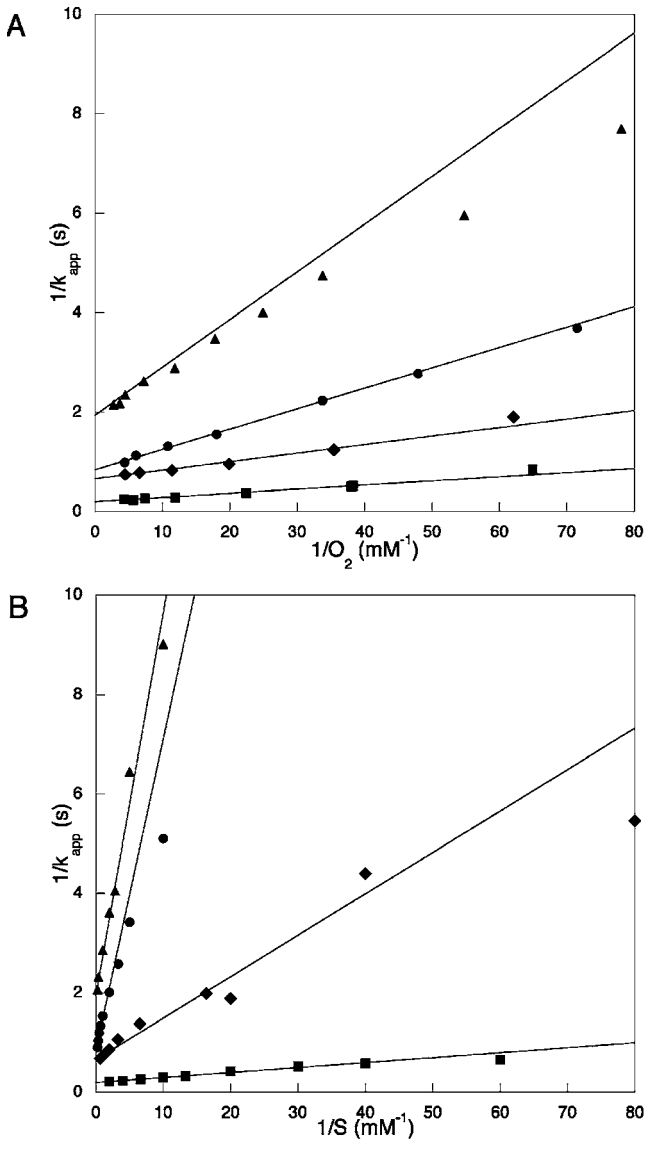

Figure 2. Double reciprocal plots with varying oxygen (A) and substrate (B) for wild-type and mutant TauD. In both panels: ■, wild-type; ♦, F159L; ●, F159V; ▲, F159A. Lines were generated using parameters from nonlinear fits to the Michaelis−Menten equation to avoid overweighting of the low concentration points common in double reciprocal fits.

k_{cat}/K_{O_2}, obtained by direct fitting of the rectangular hyperbola for v versus $[O_2]$, are summarized in Table 1 and serve as a frame of reference for the impact of mutation on substrate chemistry discussed below.

Steady-State Partial Reaction with Substrate. The steady-state parameter $k_{cat}/K_m(S)$ was determined for wild-type and F159 mutant forms of TauD to evaluate the impact of mutations on the binding of prime substrate. This is relatively straightforward, as the measurements were made at saturating dioxygen concentrations, effectively making the oxygen binding step ($k_{on}(O_2)$ in Scheme 1) irreversible. This reduces the parameter $k_{cat}/K_m(S)$ to a single rate constant, that for substrate binding ($k_{on}(S)$).[30] The greater impact of mutation on $k_{cat}/K_m(S)$ than on $k_{cat}/K_m(O_2)$ is shown by the much greater increase in the slopes of the $1/v$ versus $1/S$ as the side chain bulk is reduced (Figure 2B). The $k_{cat}/K_m(S)$ values, summarized in Table 1, indicate a nearly 100-fold diminution that is 10-fold greater than that for $k_{cat}/K_m(O_2)$. This result, where a larger active-site cavity results in a slower substrate binding rate, may initially seem counterintuitive. However, substrate must be bound in a productive fashion in order to stimulate the "substrate-triggered" binding of dioxygen. In light of this, it is clear that hydrophobic bulk at position 159 in TauD facilitates the productive positioning of substrate to an off-metal pocket in the active site.

Steady-State Reaction under Saturating Conditions of Substrate and Oxygen. The data discussed above also yielded the maximal rate of oxygen uptake, k_{cat}. Determination of the same parameter in the presence of 1,1-dideutero substrate allows the calculation of the kinetic isotope effect ($^Dk_{cat}$), where $^Dk_{cat} = k_{cat}(H)/k_{cat}(D)$. As shown in Table 1, k_{cat} diminishes only ~10-fold upon substitution of F159 by alanine, indicating that while the residue is important to enzyme turnover, it is not crucial. For a residue predicted to be critical for hydrogen transfer, the most likely explanation for the trends in k_{cat} is the kinetic importance of steps other than C−H bond cleavage.

The latter can be assessed from the magnitude of $^Dk_{cat}$, which may be expected to increase across the mutant series as chemistry becomes more rate-determining.[31] We note that the deuterium isotope effect (after correction for uncoupling, see below) for WT enzyme using taurine as substrate at pH 7.6 and 5 °C has been reported to be decreased from an intrinsic value of ca. 58 to approximately 18 under steady-state turnover conditions,[23] attributed to slow product (succinate) release.[29] However, the experimental values for $^Dk_{cat}$ with the mutant enzymes and *N*-methyltaurine as substrate (Table 1) get smaller as the rates decrease. This trend can be understood in the context of the mutant series causing an increased partitioning away from productive hydrogen atom transfer toward the unproductive uncoupled reaction; this has the impact of driving the size of the $^Dk_{cat}$ toward unity. As discussed in Materials and Methods, the experimentally determined kinetic isotope effects can be corrected to represent isotope effects for product formation using the previously determined values for $[SO_3^{2-}/O_2]^H/[SO_3^{2-}/O_2]^D$ (1.4 ± 0.1, 4.6 ± 0.6, 25 ± 3, and ≥21 for wild-type, F159L, -V, and -A, respectively). Note that the reaction with F159A and deuterio substrate is uncoupled to such an extent that only a detection threshold could be estimated for SO_3^{2-} production.[27] This makes correction of the experimental isotope effect for F159A unreliable, providing only a lower limit of 70 for the fully coupled isotope effect. Despite the poor ability to determine $^Dk_{cat}$(prod) for F159A, the trends in $^Dk_{cat}$(prod) for WT versus F159L and F159V are in the direction expected for an increasing reduction in the rate constant for hydrogen abstraction.

Stopped-Flow Kinetic Studies. Due to the limitations on steady-state measurements indicated above, stopped-flow measurements were undertaken to estimate intrinsic KIEs, as previously reported using WT enzyme and taurine as substrate at 5 °C.[23] The accumulation and decay of a species absorbing at 318 nm reports on the formation and decay of the Fe(IV)═O species.[17] In Figure 3, we show the comparative protio and deuterio kinetic traces at 318 nm for WT (A), F159L(B), and F159V(C) with *N*-methyltaurine as substrate. The resulting values for k_{decay} are summarized in Table 2. Comparison of the k_{decay} for *N*-methyltaurine (21 s^{-1}, 10 °C) to taurine (13 s^{-1}, 5 °C)[23] reinforces the steady-state intimation that methylation of the amino group would not impact substrate activation substan-

(30) Cleland, W. W. *Biochemistry* **1975**, *14*, 3220–3224.

(31) Northrop, D. B. *Biochemistry* **1981**, *20*, 4056–4061.

Table 1. Steady-State Parameters for WT TauD and F159 Variants

enzyme	$k_{cat}/K_m(O_2)$ (M^{-1} s^{-1})	k_{cat}/K_m(substrate) (M^{-1} s^{-1})	k_{cat} (s^{-1})	$^{D}k_{cat}$	$^{D}k_{cat}$(prod)
wild-type	$(1.2 \pm 0.2) \times 10^{5}$[a]	$(1.0 \pm 0.1) \times 10^{5}$[a]	5.0 ± 0.2[a]	8.3 ± 0.4	11.5 ± 0.7
F159L	$(5.8 \pm 0.5) \times 10^{4}$	$(1.2 \pm 0.2) \times 10^{4}$	1.52 ± 0.07	8.6 ± 0.7	39 ± 4
F159V	$(2.4 \pm 0.2) \times 10^{4}$	$(1.6 \pm 0.2) \times 10^{3}$	1.19 ± 0.03	4.6 ± 0.2	120 ± 20
F159A	$(1.2 \pm 0.1) \times 10^{4}$	$(1.3 \pm 0.1) \times 10^{3}$	0.52 ± 0.01	3.3 ± 0.1	≥ 70

[a] From ref 26.

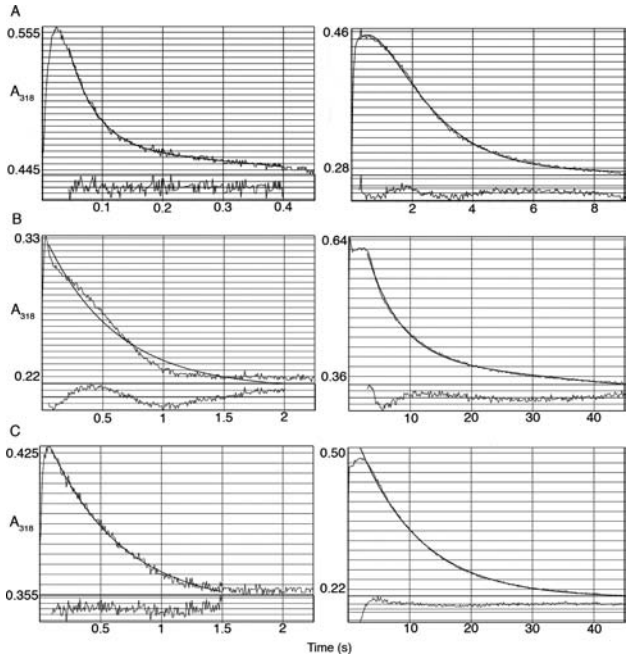

Figure 3. Stopped-flow traces for the decay of the Fe(IV)═O species in TauD for protio (left) and deuterio (right) *N*-methyltaurine. (A) WT enzyme, (B) F159L, and (C) F159V. Plots are A_{318} versus time (s) with fits as described in Materials and Methods. The residuals of the fits are shown below. These examples illustrate the range of goodness of fit in individual kinetic traces. The final rate constants and their attendant errors are the average of multiple (ca. 10) kinetic runs (Table 2).

Table 2. Stopped-Flow Parameters for WT TauD and F159 Variants

enzyme	substrate[a]	k_{decay} (s^{-1})	k_{prod} (s^{-1})	$^{D}k_{prod}$
wild-type	H	21 ± 1	21 ± 1	
	D	0.48 ± 0.08[b]	0.35 ± 0.06	60 ± 11
F159L	H	1.80 ± 0.11[b]	1.31 ± 0.09	
	D	0.188 ± 0.004	0.030 ± 0.002	44 ± 4
F159V	H	0.81 ± 0.04[b]	0.41 ± 0.03	
	D	0.100 ± 0.002	$(2.0 \pm 0.5) \times 10^{-3}$	200 ± 50

[a] H and D refer to 1,1-[$^{1}H_2$]- and 1,1-[$^{2}H_2$]-2-methylaminoethane-1-sulfonic acid, respectively. [b] From ref 27.

tially. Additionally, the size of the intrinsic KIE appears similar when comparing taurine (KIE of 58) to *N*-methyltaurine (see below).

Under conditions where all oxygen chemistry is fully coupled to product formation, the value of k_{decay} of the Fe(IV)═O species corresponds directly to the rate of hydrogen atom abstraction (k_H in Scheme 1). However, as in the steady-state, uncoupling results in inflated values for k_H, necessitating a correction to produce rate constants and isotope effects that reflect substrate functionalization. The experimentally determined decay rates (Figure 3) were thus corrected as described in Materials and Methods to generate k_{prod}. Upon substitution of F159 with V, the rate of C−H abstraction (k_{prod}) is slowed ∼50-fold (Table 2). This is on top of the already noted ca. 60-fold slowing of substrate binding (Table 1). Although these two steps are both related to substrate binding and reactivity, they are separated by an irreversible step (Scheme 1) and, thus, are never expressed on a single kinetic parameter. Nonetheless, the overall impact of the F159V substitution on substrate binding and C−H cleavage is a ca. 3000-fold decrease with respect to wild-type.

The impact of substrate deuteration on k_{prod} is also very informative. Of particular interest regarding the criticality of F159 to C−H bond cleavage is the elevation of the intrinsic KIE for F159V to 200 (50) in relation to the WT value of 60 (11) (Table 2). This aspect will be discussed in some detail in the section immediately following. The behavior of the F159A mutant, which is >50% uncoupled with protio substrate and ≥98% uncoupled with the deuterio substrate,[27] failed to yield a detectable KIE in the comparative rates of k_{decay} (data not shown), and hence, no effort was made to estimate intrinsic KIEs with this mutant. It is clear that, as uncoupling becomes extreme, it no longer becomes possible to apply a correction factor to obtain reliable values for intrinsic KIEs.

Protein Control of Hydrogen Tunneling in the TauD Active Site. The very large size of the KIE in the TauD reaction, first measured by Price et al.,[23] led to the conclusion of a role for hydrogen tunneling in this reaction. The data presented herein expand this finding and provide insight into the role of TauD in facilitating the hydrogenic wave function overlap between substrate and the active-site Fe(IV)═O. For systems with KIEs as large as those seen with TauD, an analytical rate expression for a nonadiabatic tunneling process can be written:[4]

$$k_{tun} = (\text{Const}) \exp\{-(\Delta G^\circ + \lambda)^2/(4\lambda RT)\} \times \int_{r_1}^{r_0} \exp^{-m_H \omega_H r_H^2/2\hbar} \exp^{-E_X/k_B T} \, dX \quad (5)$$

According to this treatment, the factors that control tunneling are contained in three exponential terms; first, there is the Marcus expression, derived originally for electron tunneling and dependent on the environmental reorganization, λ, together with the reaction driving force, ΔG°; second is the Franck−Condon overlap term, dependent on the tunneling particle's mass, m_H, frequency, ω_H, and the distance over which the particle transfers (r_H). Lastly, there is integration of the Franck−Condon overlap term over a range of internuclear distances, described by a barrier, E_X, that reflects the ease or difficulty of protein altering the initial internuclear distance.

According to this treatment, the final magnitude of the measured isotope effect is a trade-off between the initial distance between the heavy atoms of the hydrogen donor and acceptor and the ability of the active site to further reduce this distance via a distance sampling process. It should be pointed out that what is referred to as the initial internuclear distance is generally not the van der Waals distance seen in static pictures of enzyme active sites, but rather reports on shorter internuclear distances achieved via a prior search of a protein's conformational space for the conformational substates most amenable to tunneling. Previous studies of the impact of site-specific mutagenesis have

frequently focused on the temperature dependence of the KIE, showing a trend away from largely temperature-independent KIEs for well-organized enzyme active sites to more temperature-dependent KIEs that reflect a greater role for distance sampling once the active-site structure has been perturbed.[1,5]

The present study is focused primarily on the impact of site-specific mutagenesis on the magnitude of the KIE. In the majority of studies where the KIE has been interrogated following site-specific mutagenesis, the size of the KIE is fairly invariant at a single, physiologically relevant temperature, attributed directly to the ability of the protein to compensate for an increased initial internuclear distance by a greater role for active-site distance sampling. With regard to the data available for TauD, the temperature of the steady-state data, 30 °C, is likely to be more relevant to comparison of the magnitude of KIEs at a physiologically relevant temperature, while the single transient data at 10 °C allow a more direct measure of the intrinsic KIEs. However, using the combined data sets for F159L and F159V at 10 and 30 °C provides the information we need for evaluating the impact of active-site geometry on tunneling in this enzyme system.

Beginning with the F159L, it can be seen that the KIE on k_{cat}(prod) (30 °C) is equal to the KIE on k_{prod} (10 °C). Since the KIE is expected to be unaltered or to increase with a decrease in temperature, comparison of the measurements shows that k_H has become rate-limiting for k_{cat}(prod) for F159L at 30 °C and that the KIE is fairly insensitive to temperature. It appears that the 10-fold reduction in k_{prod} for F159L in relation to WT is not so great as to increase the size of the $^{D}k_{prod}$ nor to introduce a significant temperature dependence to the KIE. The case for F159V, however, is quite different, indicating a greatly elevated KIE at 30 °C that may undergo even further elevation at 10 °C. Given the respective errors in the F159V KIEs at the two temperatures, it is premature to conclude the degree of temperature dependence of the KIE. However, it is very evident that the KIE for F159V is elevated 2- to 4-fold in relation to an average intrinsic KIE of 52 for WT and F159L.

Hammes-Schiffer and co-workers have developed analytical expressions to relate the magnitude of vibronic coupling between donor and acceptor vibronic states (u and v, respectively), according to eq 6:[32,33]

$$V_{uv}(R) = V^{\circ}_{uv} \exp[-\alpha_{uv}(R - \bar{R}_u)] \quad (6)$$

where V°_{uv} is the vibronic coupling at $R = R_u$ and α is the proportionality factor that relates internuclear distance to coupling efficiency. The value of α_H is thought to be in the range of ca. 25 Å^{-1}, much larger than the proportionality constant of ca. 1 Å^{-1}, which describes the distance dependence of wave function overlap between donor and acceptor for tunneling of the much lighter electron. The expression in eq 6 can be expanded to separate the electronic coupling, V_{el}, from wave function overlap, S_{uv}, to give eq 7:

$$V_{uv}(R) = V_{el}S_{uv}(R) \quad (7)$$

$$S_{uv}(R) = S^{\circ}_{uv} \exp[-\alpha_{uv}(R - \bar{R}_u)] \quad (8)$$

The expression for the KIE follows from eq 8 to give

$$\mathrm{KIE} \sim (S_H/S_D)^2 \exp\left\{\frac{2k_BT}{M\omega^2}(\alpha_H^2 - \alpha_D^2)\right\} \quad (9)$$

where k_B is the Boltzmann constant and M and ω are the mass and frequency of the heavy atom gating motion. Under conditions where gating plays a significant role, the KIE becomes reduced by the exponential term, which will be less than unity due to the greater value of α_D than α_H. The latter follows directly from the larger mass and smaller wavelength for deuterium that introduces an even greater sensitivity to small distance changes than for protium.

The above approach provides a conceptual framework for understanding how gating reduces the size of the experimental KIE. Applying this framework to the current case of TauD, we find that the WT and F159L are able to reduce the active-site internuclear distance of the substrate and Fe(IV)═O, while the F159V variant cannot do this very well if at all. The reduction in distance in WT and F159L could, in fact, arise from either a viable conformational sampling process (preorganization) or during the reorganization process represented in eq 5 and eqs 6−9 that describe the local adjustments in energy and distance that provide for efficient hydrogen transfer. Given the position of the F159 side chain in TauD, directly behind the bound substrate, it is expected that a portion of the observed impact of F159V will be on the reorganization, implying that the relatively modest loss of bulk that occurs in the F159V variant disrupts the potential for effective distance sampling.

Independent of the precise physical origin of the effects reported herein (preorganization, reorganization, or a combination thereof), we conclude that the progression from Phe to Val is highly deleterious to the active site. On the surface, it might appear that the sensitivity of TauD to alteration in active-site packing is greater than that reported previously for SLO-1 since the exaggerated KIEs arise for the Val variant with TauD versus the Gly substitution in SLO-1. However, two considerations argue against such a conclusion. First, the mutation of I553 in SLO-1 takes place at a residue ca. 15 Å from the active-site iron, such that greater changes in the interim packing may be necessary to impact the C−H abstraction.[12] An even more likely explanation emerges, however, from a comparison of the actual changes in side chain bulk that leads to the "break" from native behavior. As illustrated in Scheme 2, the

Scheme 2[a]

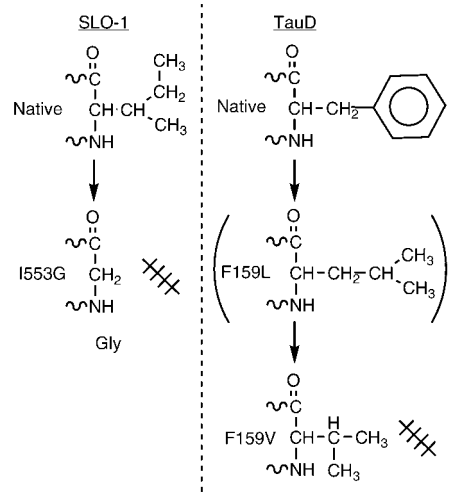

[a] Comparison of the structural change in SLO-1 (left) vs TauD (right) that leads to the significant elevation of the intrinsic deuterium isotope effect observed for I553G in SLO-1 and F159V in TauD.

(32) Hatcher, E.; Soudackov, A.; Hammes-Schiffer, S. *Chem. Phys.* **2005**, *319*, 93–100.
(33) Hammes-Schiffer, S.; Hatcher, E.; Ishikita, H.; Skone, J. H.; Soudackov, A. V. *Coord. Chem. Rev.* **2008**, *252*, 384–394.

extent of perturbation may be quite similar in proceeding from native SLO-1 to Gly, as from native TauD to Val. These results raise the very interesting possibility regarding the degree to which protein active sites can tolerate packing defects, suggesting reasonable tolerance to the production of some empty space, followed by a significant break in kinetic behavior when the perturbation exceeds a certain limit. While we do not yet have a structure for the F159V variant of TauD, the X-ray structure of the SLO-1 I553G was found to be essentially identical to the wild-type enzyme, precluding a collapse of the protein around the empty space produced by mutation or the filling up of this space with detectable waters.[12] The latter led to the conclusion of a primary impact of side chain deletion on protein dynamics. A similar explanation seems likely for the TauD F159V variant, implying a decreased capacity of the altered protein to sustain sufficient flexibility to overcome the increased distance between the C-1 of substrate and the metastable Fe(IV)═O hydrogen atom acceptor.

JA909416Z